

Mode Grüneisen parameter dispersion relation of RbI determined by neutron scattering*

O. Blaschko and G. Ernst

*1. Physikalisches Institut der Universität Wien, Strudlhofgasse 4, A-1090, Vienna, Austria
and Österreichische Studiengesellschaft für Atomenergie G.m.b.H., Lenaugasse 10, A-1082
Vienna, Austria†*

G. Quittner

*Österreichische Studiengesellschaft für Atomenergie G.m.b.H., Lenaugasse 10, A-1082
Vienna, Austria*

W. Kress† and R. E. Lechner

*Institut Laue-Langevin, B.P. 156, 38042 Grenoble-Cedex, France
(Received 12 August 1974)*

Inelastic-neutron-scattering measurements of 43 mode Grüneisen parameters for the $[00\xi]$, $[\xi\xi0]$, and $[\xi\xi\xi]$ directions of RbI are reported. These "mode γ 's" were determined to an accuracy of 2 to 10% of the Grüneisen-parameter range (about -2 to $+3$). Comparison is made and good agreement is found with the results obtained using a breathing shell model which was extended to include the third-order anharmonic interactions. The third-order parameters including those due to electronic polarization effects are determined.

I. INTRODUCTION

For the study of anharmonic effects in lattice dynamics it is convenient to divide the anharmonic interactions into two parts: a deformation part arising from the change in force constants due to a deformation of the crystal lattice induced by thermal or external stress and an interaction part related to the anharmonic coupling of one phonon with all other phonons of the crystal at a given temperature.¹ The anharmonic-coupling parameters of both parts are, however, related. Since at present the potential energy $\phi(\vec{r})$ is not sufficiently well known for alkali halides, harmonic- as well as anharmonic-coupling parameters have to be determined from experiments. In addition to the harmonic-coupling coefficients, inelastic-coherent-neutron-scattering measurements of phonons can provide information about the anharmonic-coupling parameters as well. One may consider three types of measurements.

(a) The study of the temperature dependence of phonons at constant pressure: Owing to thermal stress and the changing number of excited phonons, both the deformation part and the interaction part will change. The analysis of the phonon shift and damping can provide the coupling coefficients at least to fourth order, since the contributions of the third- and fourth-order diagrams are of the same order of magnitude.¹ For each phonon investigated, however, summations over the whole Brillouin zone are involved. Therefore numerical calculations using a realistic model for the lattice dynamics, e.g., of the shell-model type,² including the Coulomb anharmonicities and the anharmonic interactions which involve the dipole moments, are extremely difficult.

(b) The study of the temperature dependence at constant volume will provide information about the interaction part alone. Apart from experimental difficulties, similar numerical problems as in (a) arise.

(c) The method we have chosen consists in studying the pressure-dependent phonon shifts at constant temperature, which give information about the deformation part alone. A few measurements of this kind have been done in the past.^{3,4,10} We have applied a hydrostatic pressure of 3 kbar in order to achieve an isotropic deformation of the RbI crystal. Such measurements can easily be analysed in terms of a model including polarizabilities and Coulomb interactions⁵⁻⁷ to determine the coupling parameters of third order.

The analysis of our experimental results is based on the renormalized harmonic approximation¹ where the harmonic-coupling parameters depend only on the equilibrium positions of the ions at a given temperature and a given external strain. In this approximation the third-order coupling parameters are the coefficients of the linear terms in the expansion of the second-order coupling parameters with respect to the deformation. The validity of the renormalized harmonic approximation is not changed if external strain is applied at constant temperature. Within this approximation a good description of the measured phonon dispersion curves in alkali halides is provided, if a model is used which allows for electronic polarization effects.² For the present investigation a breathing shell model⁸ (BSM) was used.

RbI was chosen because it has many interesting properties: It is the least stable alkali halide showing NaCl structure at atmospheric pressure, and it exhibits a polymorphic phase transition to

the CsCl structure at only 3.6 kbar.⁹ Both ions are strongly polarizable.¹⁰ The mode Grüneisen parameter for the long-wavelength transverse-acoustic phonons in the [100] direction of the Brillouin zone has a large negative value¹¹ compared with other alkali halides and the thermal-expansion coefficient is negative below 8 K.¹²

II. EXPERIMENTAL

Using the three-axis spectrometer IN2, at the high-flux reactor in Grenoble, phonon measurements were carried out on a cylindrical (30-mm-diam, 50-mm-high [110]-axis) RbI crystal along the symmetry directions [00 ξ], [$\xi\xi$ 0], and [$\xi\xi\xi$] at 3 kbar and at atmospheric pressure. The pressure technique has been described previously.¹³ Grüneisen parameters

$$\gamma(q; j) = \left. \frac{-d \ln \omega(\vec{q}, j)}{d \ln V} \right|_T$$

were obtained from the frequency shifts and the volume change ($\Delta V/V$ was calculated from the Bragg-angle changes to -0.024 ± 0.001) observed under pressure. These "mode γ 's" could be determined to an accuracy of 2 to 10% of the Grüneisen-parameter range (-2 to $+3$).

Most of the information was obtained on the acoustic branches. For this part of the measurements bent pyrolytic-graphite crystals (PG) were used as monochromators in conjunction with a pyrolytic graphite filter and pyrolytic graphite as analyzer. The horizontal collimations were, in the sequence from reactor to detector, 60', 25', 56' and 56'. Constant- Q scans with fixed k_0 ($k_0 = 2.67 \text{ \AA}^{-1}$) were used throughout this part of the measurements. About 40 different phonon pairs were measured in this way, many of them in two different Brillouin zones. For the measurement of optical phonons Cu(111) monochromators were used together with a PG filter in front of the PG analyzer. Six TO phonons were studied, but no LO phonons. The selection of measurement points in reciprocal space was guided in the usual way by consideration of the phonon structure factor obtained from the model calculation.⁵

The transverse branches [00 ξ] and [$\xi\xi$ 0] did not present any serious problems. In the transverse [$\xi\xi\xi$] as well as in the longitudinal branches peak distortions were encountered, which make the evaluation of peak shifts more difficult. Another difficulty arose with small- q phonons. In spite of the large counting rates, the errors in the Grüneisen parameters rise steeply if the phonon peak is superimposed on the slope of an incoherent elastic peak. Owing to this effect the limit of feasibility towards smaller q 's was actually about $q = 0.1$ to 0.15 in any direction. The problems arising in

the evaluation of the peak shifts in these cases are discussed in detail in Sec. III.

III. DETERMINATION OF PHONON FREQUENCY SHIFTS FROM THE EXPERIMENTAL PHONON GROUPS

The main problem in deriving phonon frequency shifts from the experimental phonon groups is the fact that, with the exception of the optical phonons, the phonon shifts are small compared to the width of the individual group. In the classical optical sense the shifted and the unshifted phonon groups are not "resolved." It is therefore essential that the shift determination is treated as a relative measurement; i. e., the absolute values of the two phonon energies do not have to be known to a comparable accuracy.

The essential basis of the evaluation is the "templet hypothesis." According to this hypothesis the phonon group does not change its shape when pressure is applied, but is merely shifted along the energy axis like a rigid templet. This templet is pinned rigidly to the "ideal phonon" and the shift of the templet is exactly equal to the shift of this ideal phonon. It is this shift which we are comparing with the phonon shifts calculated on the basis of our model.

In the field of neutron scattering a hypothesis of this kind seems to have been applied for the first time by Brockhouse in his measurements of Kohn anomalies in lead.¹⁴ Some of the present authors have used this hypothesis in several previous measurements of Grüneisen parameters.³

It is important to note that the ultimate limits of accuracy in shift measurements, once the counting statistics are sufficiently good, is given by the validity of the templet hypothesis. In the analysis of phonon-group shifts we therefore use the templet hypothesis with due consideration of conditions which might violate its validity. The following effects can limit the validity of the hypothesis:

(i) Spurious peaks which are submerged in the main peak, and are large enough to have an influence. Spurious-peak search programs have been used, similar to those in Ref. 15. Another means which has been applied is a visual comparison of both groups and control of the integrated intensities.

(ii) Uncertainties in the background subtraction.

(iii) Change of the phonon peak due to pressure-induced changes in $\nabla_q \omega(\vec{q})$. This effect is of second order due to the smallness of shifts.

The [00 ξ] and [$\xi\xi$ 0] longitudinal- and transverse-acoustic branches present little difficulty (Fig. 1) except for the low- q phonons and the turnover points of the longitudinal branches (Gaussian peak shape over a small background). Fortunately exactly these phonons are of particular importance in the comparison with our calculations. The gen-

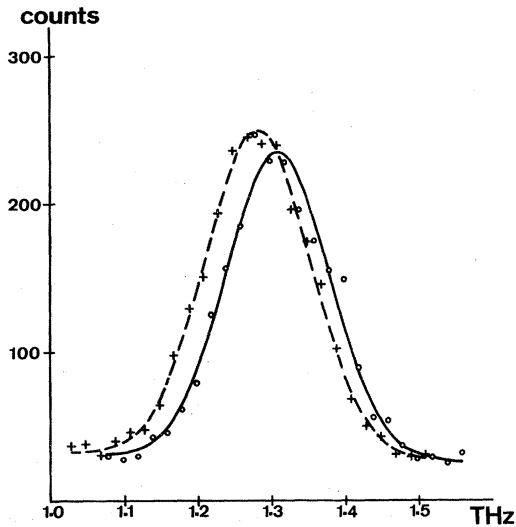


FIG. 1. Measured phonon groups for TA [114] at atmospheric pressure (○) and at 3 kbar (+). The full lines are fits of Gaussians to the experimental points taking into account a linear background.

eral procedure applied in the shift determination was a least-squares fit to each of the two groups consisting of a Gaussian for the main peak and a background (either a constant or a straight line and/or another Gaussian centered around zero or with a free position). When the background parameters of the neutron groups measured at zero and at high pressure gave satisfactory agreement, the differences of the fitted peak positions were taken as the shift. When there were considerable differences in these parameters (exception rather than the rule) the influence of the uncertainty there-of was estimated and added to the error.

By and large, the least-squares fits automatically reflect the uncertainties stemming, e.g., from the background subtraction. In most cases good fits to the experimental neutron groups were obtained. An exception are the small- q phonons where the statistics are extremely good and non-Gaussian shapes are superimposed on a large background. Here statistical inaccuracies are no longer the main problem. In these cases we are dealing with systematic errors; i.e., we approach the validity of the templet hypothesis. Part of the increase of the final error at small q is due to the use of a Gaussian for the main peak and could be remedied by using an appropriate different peak shape. This would, however, not solve the problem of background subtraction; we feel the sharp increase of the error is a fair indication of the true uncertainty towards small q 's (below about $q = 0.15$). A true improvement for small q 's would require a better resolution.

Some of the measurements had to be excluded

from evaluation either already by inspection or after unsuccessful attempts along the above lines. The results are given in Table I. The phonon pairs 19, 36, 37 are marginal cases in this respect but are of less importance in the comparison with our calculations.

An ultimate but very important justification of

TABLE I. Values of the mode Grüneisen parameters $\gamma(\vec{q}, j)$ measured at the points Q in the (110) plane of the reciprocal lattice.

No.	ξ	Pol(j)	Q			$\gamma(\vec{q}, j)$
[00 ξ]						
1	0.2	TA	2	2	-0.2	-0.98±0.24
2	0.3	TA	2	2	-0.3	-1.09±0.12
3	0.5	TA	2	2	-0.5	-1.32±0.11
4	0.6	TA	2	2	-0.6	-1.58±0.12
5	0.7	TA	2	2	-0.7	-1.64±0.15
6	0.9	TA	2	2	-0.9	-1.77±0.15
7	1.0	TA	2	2	-1.0	-1.53±0.15
8	0.2	LA	0	0	4.2	1.84±0.32
9a	0.3	LA	0	0	4.3	2.60±0.27
9b	0.3	LA	0	0	2.3	2.66±0.21
10	0.4	LA	0	0	4.4	2.27±0.15
11	0.5	LA	0	0	4.5	2.51±0.18
12	0.7	LA	1	1	4.3	0.33±1.17
13	0.8	LA	1	1	4.2	-0.01±0.10
14	0.9	LA	1	1	4.1	-0.58±0.09
15a	1.0	LA	1	1	4.0	-0.84±0.10
15b	1.0	LA	1	1	2.0	-0.91±0.20
16	0	TO	3	3	-1	2.23±0.20
17	0.5	TO	3	3	-0.5	2.49±0.35
18	1.0	TO	3	3	0	2.46±0.27
[$\xi\xi 0$]						
19	0.1	T ₁ A	0.1	0.1	4	-0.68±0.68
20	0.2	T ₁ A	0.2	0.2	4	-1.28±0.11
21a	0.3	T ₁ A	0.3	0.3	4	-1.09±0.11
21b	0.3	T ₁ A	0.3	0.3	2	-1.03±0.14
22a	0.4	T ₁ A	0.4	0.4	4	-1.39±0.15
22b	0.4	T ₁ A	0.4	0.4	2	-1.28±0.11
23a	0.5	T ₁ A	0.5	0.5	4	-1.37±0.10
23b	0.5	T ₁ A	0.5	0.5	2	-1.01±0.08
24a	0.6	T ₁ A	0.6	0.6	4	-1.07±0.06
24b	0.6	T ₁ A	0.6	0.6	2	-0.97±0.08
25a	0.7	T ₁ A	0.7	0.7	4	-0.97±0.07
25b	0.7	T ₁ A	0.7	0.7	2	-0.95±0.14
26a	0.9	T ₁ A	0.9	0.9	4	-0.96±0.09
26b	0.9	T ₁ A	0.9	0.9	2	-1.07±0.17
15a	1.0	T ₁ A	1	1	4	-0.84±0.10
15b	1.0	T ₁ A	1	1	2	-0.91±0.20
[$\xi\xi 0$]						
27	0.2	LA	2.2	2.2	0	1.89±0.26
28	0.3	LA	2.3	2.3	0	1.95±0.31
29	0.4	LA	2.4	2.4	0	1.90±0.31
30	0.7	LA	2.3	2.3	1	0.88±0.09
31	0.8	LA	2.2	2.2	1	0.90±0.09
32	0.9	LA	2.1	2.1	1	-0.74±0.17
(7)	1.0	LA	2	2	-1	-1.53±0.15
33	0	T ₁ O	1	1	5	2.24±0.26
34	0.5	T ₁ O	0.5	0.5	5	2.71±0.34
35	1.0	T ₁ O	0	0	5	2.93±0.29
[$\xi\xi\xi$]						
36	0.1	TA	2.1	2.1	3.9	0.54±0.53
37	0.15	TA	2.15	2.15	3.85	1.03±0.28
38	0.25	TA	2.25	2.25	3.75	2.26±0.28
39	0.35	TA	2.35	2.35	3.65	2.05±0.28
40	0.45	TA	2.45	2.45	3.55	2.29±0.22
41	0.15	LA	2.15	2.15	2.15	1.91±0.28
42	0.25	LA	2.25	2.25	2.25	1.76±0.18
43	0.35	LA	2.35	2.35	2.35	1.52±0.15

the validity of the evaluation is given by (a) the agreement of the γ values for phonons measured in two Brillouin zones (numbers 9, 15, 21, 26, in Table I), (b) the continuity of the γ 's as a function of wave vector \vec{q} , and (c) the qualitative agreement with all previous Grüneisen parameter calculations,^{5-7,16} e. g., the fast decrease from large positive to negative values in the $[00\xi]$ and $[\xi\xi 0]$ longitudinal branches, the negative values of the $[00\xi]$ and $[\xi\xi 0]$ transverse branches as opposed to positive values of γ 's in all other branches.

IV. CALCULATIONS

In the calculations we have used a breathing-shell model where axially symmetric force constants to first (A_{12}, B'_{12}) and second nearest neighbors (A_{22}, B_{22}) were taken into account. (1 labels Rb^+ ions, 2 labels I^- ions.) These forces were assumed to act only via the shells. The shells were coupled to their own cores by the force constants k_1 and k_2 . The isotropic deformability of the shells was characterized by the constants $g_1 = E_1 k_1$ and $g_2 = E_2 k_2$. The ionic charge is Z and the shell charges Y are assumed to be equal.¹⁷ With this model a quite satisfactory description of the measured¹⁸ phonon dispersion curves is possible, as was shown by one of the authors in a previous paper⁵ where the details are given.

The third-order coupling parameters ($\dot{A}_{12}, \dot{B}'_{12}, \dot{A}_{22}, \dot{B}_{22}, \dot{Y}, \dot{k}_1, \dot{k}_2$) of this model are obtained from the isothermal isotropic pressure derivatives of the long-wavelength data (i. e., the three elastic constants c_{ij} , the dielectric constants ϵ_0 and ϵ_∞ , the reststrahlen frequency ω_R , and the ionic polarizabilities α_I and α_{Rb}) in a similar way as are the harmonic parameters from the undifferentiated data.⁵ The only parameter which cannot be determined from the long wavelength data is the derivative \dot{Z} of the ionic charge. Here \dot{A}_{12} , etc., denote the derivatives ($-d \ln A_{12} / d \ln v$)_{T, r_0}, etc. In Ref. 5 \dot{Z} was found to affect strongly one of the acoustic mode Grüneisen parameter branches in the region around the X point. In the $[100]$ direction this branch corresponds to the LA, in the $[110]$ direction to the T_1A phonons. In that previous calculation the value of $\dot{Z} = -1.47$ had been

TABLE II. Input parameters for the calculation of the mode Grüneisen parameters. The values are the same as in Ref. 5, except for γ_{44} and \dot{Z} .

$\gamma_{11} = 2.55,$	$\gamma_{44} = -1.20,$	$\left. \frac{d \ln \epsilon_0}{d \ln v_a} \right _T = 1.41$
$\gamma_{12} = 1.86,$	$\gamma_{TO}(\Gamma) = 2.37,$	$\left. \frac{d n_\infty}{d \ln v_a} \right _T = -0.407$
$\dot{Z} = 0.0,$	$\left. \frac{d \alpha_{Rb}}{d \ln v} \right _T = 0.286 \text{ \AA}^3,$	$\left. \frac{d \alpha_I}{d \ln v_a} \right _T = 3.438 \text{ \AA}^3$

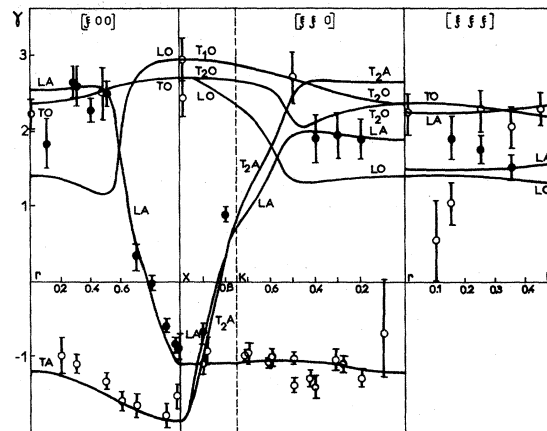


FIG. 2. Dispersion of the mode Grüneisen parameters. Full lines: calculation; open circles, full circles: measurements with error bars for the transverse and longitudinal branches, respectively.

adjusted so as to obtain agreement with the thermal-expansion coefficient at $T = 283^\circ \text{K}$. The results of the present experiment allow us to determine \dot{Z} in a more direct way. Best agreement with the measured mode Grüneisen parameters is now found with $Z = 0.0$. In addition, our measured mode Grüneisen parameters for the transverse-acoustic branch (Table I) in the $[100]$ direction do not confirm the low value of -3.32 at the X point measured by Saunderson.¹⁹ In the frame of the present calculations our data give better agreement with the average of the different available ultrasonic results.¹¹ Therefore the corresponding input parameter $\gamma_{44} = -\frac{1}{6}(1 - \dot{C}_{44})$ was changed from -1.27 (chosen in Ref. 5) to -1.20 . The input data finally used in our calculation are summarized in Table II.

In general the agreement between the calculated and measured mode γ dispersion curves (see Fig. 2) is quite satisfactory. Moreover the calculation shows that the neutron results are consistent with the optical and acoustical data and that the anharmonic extension of the BSM is a useful approach for the calculation of mode Grüneisen parameters in alkali halides.

As a further check we have recalculated the linear thermal-expansion coefficient

$$\alpha(T) = \frac{k_B}{3B_T V} \sum_{a,j} \gamma(\vec{q}; j) C(T; \vec{q}; j),$$

where $C(T; \vec{q}; j)$ is the Einstein specific-heat function. The result is given in Fig. 3. In the high-temperature limit the results are now in better agreement with the measurements of Schuele and Smith²⁰ than in Ref. 5. In the low-temperature region the agreement is slightly poorer owing to the small upward shift of the TA mode Grüneisen

parameters in the [100] direction. It still remains satisfactory if we consider the approximations made for the calculation of the linear thermal-expansion coefficient.

V. DISCUSSION

Since the development of a justification from first principles for the different models used in phonon calculations is still in progress²¹ we give here only a crude qualitative picture for the interpretation of some of the anharmonic parameters given in Table III.

The leading term in the short-range repulsive interactions is \dot{A}_{12} . The force constant A_{12} arises from the overlap of the wave functions of neighboring ions. The radial part of the wave functions will in a first approximation lead to a Born-Mayer-type repulsive potential $\phi(r) = B e^{-r/\rho}$ and \dot{A}_{12} corresponds in this picture to r_0/ρ , which describes the decrease of the potential. The Coulomb contribution to the dynamical matrix can be factorized into a part depending only on the structure, which does not change if hydrostatic pressure is applied, and a prefactor containing the charges and the volume of the elementary cell. For the Coulomb interaction between the ions this prefactor is $\pm Z^2 e^2/v_a$. Its change with applied hydrostatic pressure would lead to stronger Coulomb forces if the ionic charge Z were not affected. The wave functions for an ionic crystal will not only consist of the individual wave functions of the free ions but may have mixed-in homopolar contributions arising from the exchange of the s and p electrons of Rb and I, respectively. This "exchange part" may explain the value of $0.88e$ of the Coulomb charge in RbI found within the BSM at atmospheric pressure. With increasing hydrostatic pressure the exchange part might increase, leading to a decrease of the Coulomb-charge Z compensating partly the strengthening of the Coulomb

TABLE III. Shell-model parameters and their derivatives (obtained from the input parameters given in Table I).

X		$-\frac{d \ln X}{d \ln r} \Big _T^a$	$-\frac{d \ln X}{d \ln r} \Big _T$ (present)
A_{12}	$14.40e^2/v_a$	+10.36	11.88
B_{12}	$-0.9981e^2/v_a$	15.87	19.25
A_{22}	$0.7991e^2/v_a$	11.56	14.53
B_{22}	$-0.1834e^2/v_a$	-9.798	1.76
Z	$0.8795e$	-1.473	0.00
Y	$-3.888e$	+10.30	2.59
k_1	$800.3e^2/v_a$	+21.25	5.58
k_2	$223.2e^2/v_a$	+22.96	6.63
E_1	1.000	0.000	0.000
E_2	3.000	0.000	0.000

^aSee Ref. 5.

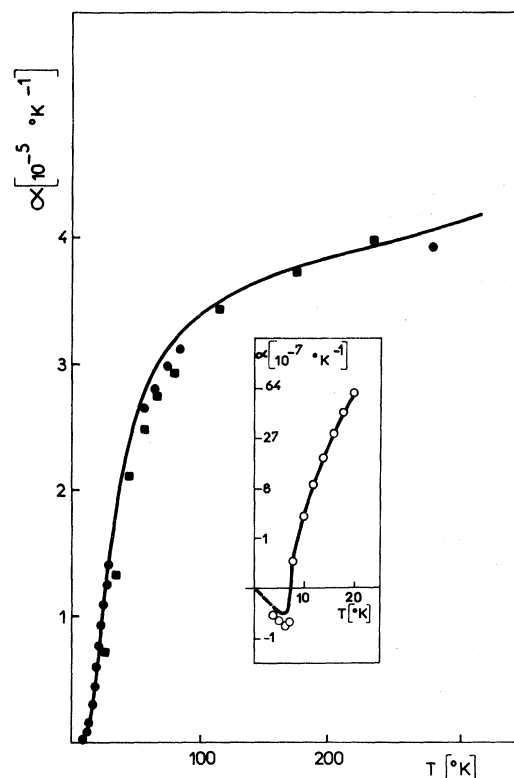


FIG. 3. Linear thermal-expansion coefficient. Full line: calculations; \circ , measurements of Refs. 12 and 20, respectively.

interaction due to v^{-1} . In Ref. 5 this effect was overestimated and both parts cancelled nearly completely. From the results of the present measurements it is found that the change in the exchange part can be neglected and the Coulomb forces increase with pressure [$-d \ln(Z^2/v_a)/d \ln r = 3.0$]. Consequently the repulsive forces are increasing faster than obtained in Ref. 5.

VI. CONCLUSION

The mode Grüneisen parameters of RbI obtained from our measurements and the present model calculations are in good agreement. In particular, the model predicts the positive and negative signs of different mode γ branches and the steep slopes of the LA [00 ξ] and [$\xi\xi 0$] branches remarkably well. This is rather encouraging since the model is constructed in such a way as to exactly reproduce for $q \rightarrow 0$ the ultrasonic and optic results. Therefore the mode Grüneisen parameters determined with different methods in different regions of the Brillouin zone are consistent within the framework of the present theory. Satisfactory agreement was found as well for the calculated and linear thermal-expansion coefficient in the

measured values of the whole temperature region between 4 and 300 °K. This indicates that the model used does not only give a realistic description of the dispersion relations of both phonons and mode Grüneisen parameters along symmetry directions, but in the whole Brillouin zone. We finally conclude that for suitable substances measurements of mode Grüneisen parameters at a high-flux reactor can give valuable information pertinent to the anharmonic lattice dynamics.

ACKNOWLEDGMENTS

We would like to thank Dr. B. Dorner for advice and P. Flores for technical assistance in the experiment. We are grateful to Dr. H. Jex and Dr. M. Müllner for providing the RbI single crystal. One of us (W.K.) is indebted to Professor H. Bilz and Professor E. Lüscher for valuable discussions and continuous support. Several of us (O.B., G.E., and G.Q.) thank the Institute Laue-Langevin for its hospitality.

*Supported in part by Fonds zur Förderung der wissenschaftlichen Forschung in Österreich.

†Correspondence should be sent to the second address.

‡Also Physik-Department E13, Techn. Universität München.

¹R. A. Cowley, *Adv. Phys.* **12**, 421 (1963); E. R. Cowley and R. A. Cowley, *Proc. R. Soc. A* **287**, 259 (1965).

²W. Cochran, *Crit. Rev. Solid State Sci.* **2**, 1 (1971).

³R. E. Lechner and G. Quittner, *Phys. Rev. Lett.* **17**, 1259 (1966); G. Quittner, S. Vukovich, and G. Ernst, *Neutron Inelastic Scattering* (IAEA, Vienna, 1968), Vol. I, p. 367; G. Ernst, *Acta Phys. Austriaca* **33**, 27 (1971); O. Blaschko, G. Ernst, and G. Quittner, *J. Phys. Chem. Solids* **36**, 41 (1975).

⁴J. R. D. Copley, C. A. Rotter, H. G. Smith, and W. A. Kamitakahara, *Phys. Rev. Lett.* **33**, 365 (1974).

⁵W. Kress, *Phys. Status Solidi B* **62**, 403 (1974).

⁶G. R. Barsch and B. N. N. Achar, *Phys. Status Solidi* **35**, 881 (1969); B. N. N. Achar and G. R. Barsch, *Phys. Status Solidi A* **6**, 247 (1971).

⁷K. V. Namjoshi, S. S. Mitra, and J. V. Vetelino, *Phys. Rev. B* **3**, 4398 (1971).

⁸U. Schröder, *Solid State Commun.* **4**, 347 (1966); V. Nüblein and U. Schröder, *Phys. Status Solidi* **21**, 309 (1967).

⁹J. Peyronneau and A. Lacam, *Bull. Bur. Nat. Météorol. Paris* **5**, 21 (1974).

¹⁰J. R. Tessman, A. H. Kahn, and W. Shockley, *Phys. Rev.* **92**, 890 (1953).

¹¹Z. P. Chang and G. R. Barsch, *J. Phys. Chem. Solids* **32**, 27 (1971); M. Gafelehbash, D. P. Dandekar, and A. L. Ruoff, *J. Appl. Phys.* **41**, 652 (1970); J. J. Fontanella and D. E. Schuele, *J. Phys. Chem. Solids* **31**, 647 (1970).

¹²G. K. White, *Proc. R. Soc. A* **286**, 204 (1965).

¹³R. Lechner, *Rev. Sci. Instrum.* **37**, 1534 (1966); O. Blaschko and G. Ernst, *Rev. Sci. Instrum.* **45**, 526 (1974).

¹⁴B. N. Brockhouse, *Phys. Rev.* **128**, 1099 (1962).

¹⁵J. R. D. Copley and B. N. Brockhouse, *Can. J. Phys.* **51**, 657 (1973).

¹⁶H. Jex, *Phys. Status Solidi B* **62**, 393 (1974).

¹⁷J. E. Hanlon and A. W. Lawson, *Phys. Rev.* **113**, 472 (1959).

¹⁸G. Raunio and S. Rolandson, *Phys. Status Solidi* **40**, 749 (1970).

¹⁹D. H. Saunderson, *Phys. Rev. Lett.* **17**, 530 (1966).

²⁰D. E. Schuele and C. S. Smith, *J. Phys. Chem. Solids* **25**, 801 (1964).

²¹S. Sinha, *Crit. Rev. Solid State Sci.* **3**, 273 (1973).